Microchimica Acta (2019) 186: 408
https://doi.org/10.1007/s00604-019-3519-1

ORIGINAL PAPER

MnO_2 nanosheets as oxidase mimics for colorimetric detection of alkaline phosphatase activity

Fengyu Tian[1,2,3] · Jing Zhou[1,2,3] · Jing Ma[3] · Siyuan Liu[3] · Bining Jiao[1,2,3] · Yue He[1,2,3]

Received: 26 January 2019 / Accepted: 19 May 2019 / Published online: 10 June 2019
© Springer-Verlag GmbH Austria, part of Springer Nature 2019

Abstract

A sensitive colorimetric method is described for the determination of the activity of alkaline phosphatase (ALP). It is based on the regulation of the oxidase-mimicking activity of MnO_2 nanosheets. In the absence of ALP, MnO_2 nanosheets are capable of catalyzing the oxidation of the colorless substrate 3,3′,5,5′-tetramethylbenzidine (TMB) by oxygen to form a blue oxidized product (TMB Ox) with an absorption peak at 652 nm. In the presence of ALP and its substrate ascorbic acid-2-phosphate, the latter is hydrolyzed to form ascorbic acid (AA). AA triggers the decomposition of MnO_2 nanosheets by reducing MnO_2 to Mn^{2+}, thereby weakening the enzyme mimicking activity of the MnO_2 nanosheets and causing a drop in absorbance. The drop in absorbance at 652 nm is related to the ALP activity in the range from 0.05–10 m-units per mL ($mU \cdot mL^{-1}$), and the detection limit is 0.05 $mU \cdot mL^{-1}$. The method was applied to the determination of ALP in spiked calf serum samples and gave satisfactory results.

Keywords Enzyme activity assay · Visual detection · Nanozyme · Ascorbic acid · Ascorbic acid-2-phosphate · 3,3′,5,5′-Tetramethylbenzidine

Introduction

Alkaline phosphatase (ALP) is an essential enzyme that can catalyze the dephosphorylation of a many substrates due to its broad substrate specificity [1]. Since an abnormal level of ALP can cause a variety of diseases in the body, it has become the most important indicator in diagnosis and therapy of diseases [2]. Therefore, sensitive and efficient monitoring of ALP activity in biological fluids is of great significance in clinical early diagnosis and effective management of illnesses.

Until now, several novel analytical strategies have been reported for ALP activity determination. They include colorimetric assays [3], fluorescence assays [4], and chemilumiescence assays [5]. Among these techniques, colorimetric assay has attracted a lot of attentions due to its unique visual detection and because it does not involve the use of highly complex apparatus. Also, numerous colorimetric methods have been developed for the detection of ALP by assisting with different nanomaterials, which include transition metal complexes, noble metal nanomaterials, ionic enzyme mimics, and so on. [6–8]. However, most of these methods have some drawbacks, including complex syntheses for phenanthroline-based transition metal complexes, high cost for noble metal nanomaterials, and poor interference ability for ionic enzyme mimics. To overcome these shortcomings, it is necessary to develop a simple and low-cost colorimetric method with high stability.

Since its appearance, MnO_2 nanosheets, as a kind of two-dimensional (2D) nanozyme, have become significant in colorimetric assay due to their unique properties, such as intrinsic oxidase-like activity, high specific surface area, good water solubility, excellent biocompatibility and greater tolerance to environmental conditions [9–11]. Compared with other nanomaterials, the preparation process of MnO_2 nanosheets

Electronic supplementary material The online version of this article (https://doi.org/10.1007/s00604-019-3519-1) contains supplementary material, which is available to authorized users.

✉ Yue He
yuehe@cric.cn

[1] Laboratory of Quality & Safety Risk Assessment for Citrus Products (Chongqing), Ministry of Agriculture, Citrus Research Institute, Southwest University, Chongqing 400712, People's Republic of China

[2] National Citrus Engineering Research Center, Chongqing, People's Republic of China

[3] College of Food Science, Southwest University, Chongqing 400712, People's Republic of China

is simple and low-cost. In addition, MnO_2 nanosheets can use the dissolved oxygen in the water to catalyze colorless substrate 3,3′,5,5′-tetramethylbenzidine (TMB) to blue oxidized product (TMB Ox), thus overcoming the requirement for hydrogen peroxide [12]. After MnO_2 nanosheets are decomposed to Mn^{2+} by reductive species (such as ascorbic acid [13], glutathione [14], and thiocholine [15]), the intrinsic oxidase catalytic activity disappears. According to the above properties, colorimetric assays based on MnO_2 nanosheets as an artificial enzyme have been successfully achieved for the detection of some important molecules such as glucose [16], ascorbic acid [13], glutathione [14], dopamine [17], and acetylcholinesterase activity [18]. These methods share the advantages of facile operation and high sensitivity. It denotes that MnO_2 nanosheets-based colorimetric strategies have high potential applicability in biosensing. However, the development of this field is still in the initial stage. Therefore, building more MnO_2-based colorimetric detection platforms for other molecules is still needed to further expand the application of MnO_2 nanosheets in biosensors.

Inspired by the above considerations, a facile and low-cost colorimetric assay is developed based on MnO_2 nanosheets for the detection of ALP activity. As illustrated in Fig. 1, in the absence of ALP, the unreacted ascorbic acid-2-phosphate cannot react with MnO_2 nanosheets. Thus, the colorless substrate TMB is oxidized and the TMB Ox with blue color is obtained. However, in the presence of ALP, ascorbic acid-2-phosphate is hydrolyzed to form ascorbic acid [4, 19]. This product reduces MnO_2 into Mn^{2+}, resulting in the losing of oxidase-mimic activity of MnO_2 nanosheets. It denotes that TMB cannot be oxidized in this process, thus the color remains unchanged. Based on the above reaction process, a new visual distinction strategy, which does not require sophisticated design and complicated instrumentation, has been established for the detection of ALP activity.

Experimental

Chemicals and instruments

Alkaline phosphatase (ALP) was obtained from Takara Biotechnology Co., Ltd. (Dalian, China) (website: http://www.takara.com.cn). In addition, ascorbic acid-2-phosphate (AAP), ascorbic acid (AA), tetramethylammoniam hydroxide (TMA·OH) and manganese chloride tetrahydrate ($MnCl_2·4H_2O$) were all obtained from Sigma-Aldrich, Inc. (Shanghai, China) (website: http://www.sigmaaldrich.com/china-mainland.html). Hydrogen peroxide (H_2O_2, 30%) was purchased from Sinopharm Chemical Reagent Co., Ltd. (Shanghai, China) (website: http://shreagent.lookchem.com). As well, 3,3′,5,5′-tetramethylbenzidine (TMB), glucose oxidase (GOx), glucose (Glu), horseradish peroxidase (HRP), glutathione reduced (GSH), L-cysteine (Cys) and urea were all obtained from Shanghai Sangon Biotechnology Co., Ltd. (Shanghai, China) (website: http://www.sangon.com). Further, the commercial ALP-kit was purchased from Beyotime. Biotechnology Co., Ltd. (Shanghai, China) (website: http://www.beyotime.com). The Tris-HCl buffer was used in the experiment consisted of 50 mM Tris-HCl (pH 9.0) and 5 mM $MgCl_2$, while the NaAc-HAc buffer consisted of 200 mM NaAc-HAc (pH 4.5). The 18.2 MΩ of deionized water used throughout the study and had been obtained from a Milli-Q water purification system.

The JEM-1200EX transmission electron microscope (JEOL, Japan) was used to take transmission electron microscopy (TEM) image. The Dimension Icon atomic force microscopy (Bruker, Germany) was then used to perform atomic force microscopy (AFM) experiment. UV-vis absorption spectra were collected from Varian Cary 50 UV-vis spectrophotometer (Palo Alto, American). The Thermo Scientific Escalab 250Xi spectrometer (Thermo Scientific, USA), with Al Kα X-ray (1486.6 eV) as the light source, was utilized to carry out characterization of X-ray photoelectron spectroscopy (XPS). All experimental data were analyzed by origin 9.0.

Preparation of MnO_2 nanosheets

Ultrathin MnO_2 nanosheets were synthesized by the previously reported method [10]. In detail, 18 mL deionized water, 87 μL TMA·OH (138 M) and 2 mL H_2O_2 (30%) were mixed together. Subsequently, 10 mL $MnCl_2$ solution (0.5938 g) was quickly added to the solution to obtain a dark brown solution. Then, the solution was stirred vigorously for overnight in the open air overnight at room temperature. After centrifuging and washing, the precipitated bulk of MnO_2 was dried at 60 °C. Lastly, 10 mg bulk of MnO_2 was dispersed in 10 mL deionized water before the solution was ultrasonic exfoliated for 2 h. The unexfoliated MnO_2 was then removed through centrifuging at low speed. On the basis of the Lambert-Beer′s Law, the concentration of the MnO_2 nanosheets solution was quantified (the molar extinction coefficient of MnO_2 nanosheets at 380 nm is 9.6×10^3 M^{-1} cm^{-1}) [20].

Optimization

To optimize the concentration of MnO_2 nanosheets, 26 μL Tris-HCl buffer, 4 μL ALP (10^4 m-units per mL, 10^4 mU·mL^{-1}) and 10 μL AAP (2 mM) were mixed and subsequently incubated for 30 min at 37 °C. Then, 156 μL NaAc-HAc buffer containing different concentrations of MnO_2 nanosheets was added into the solution. Prior to incubation for

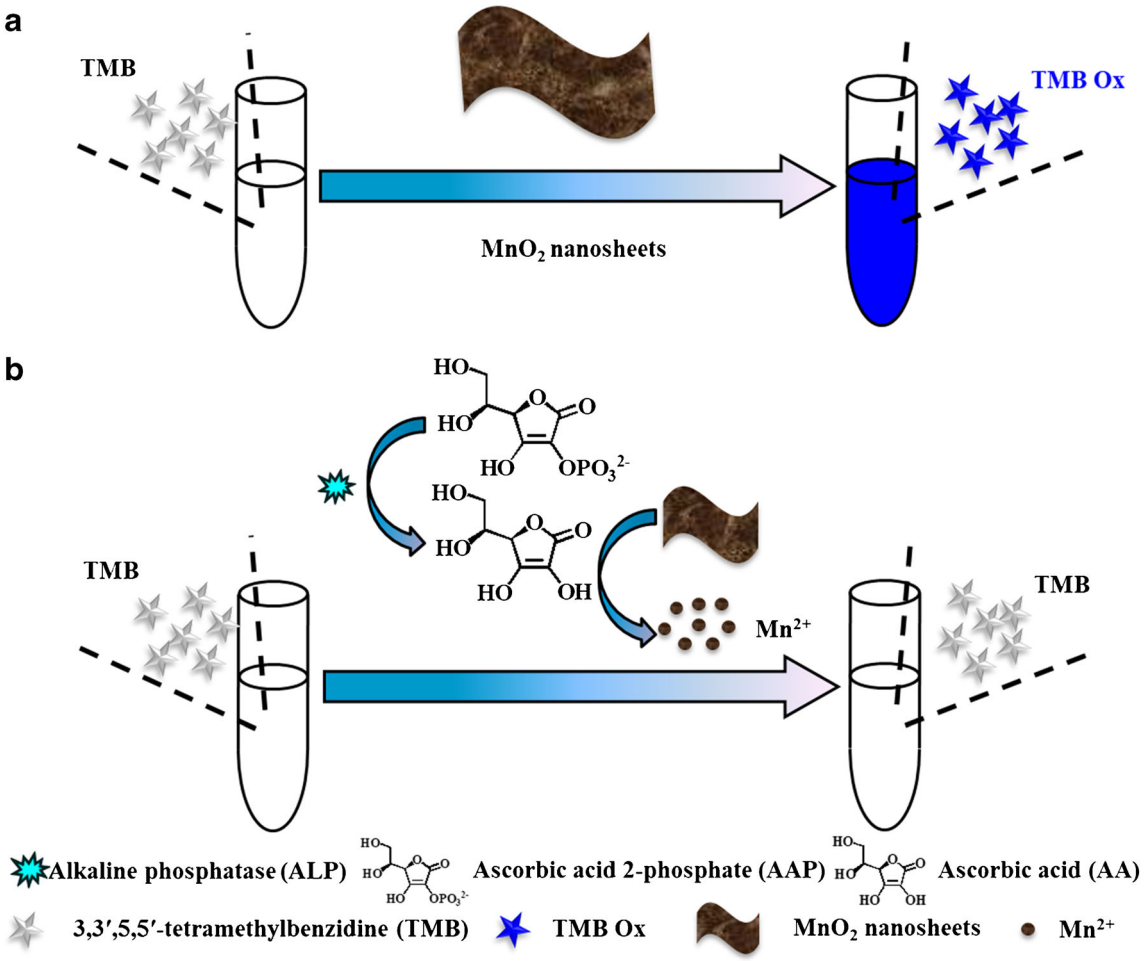


Fig. 1 Schematic of MnO_2 nanosheets-based colorimetric platform for ALP activity

5 min at room temperature, 4 μL TMB (8 mM) was added into the solution. After that, the solution was incubated for 5 min in the dark. Finally, the absorbance intensity of the solution was measured at 652 nm by Varioskan LUX microplate reader (Thermo Scientific, Vantaa, Finland) after it was transferred into the 96-well plate. Similarly, control experiments were conducted under the same conditions, except that no ALP was added. All the experiments were repeated for three times.

To optimize the concentration of AAP, series of concentrations of AAP were mixed with 4 μL ALP solution (10^4 mU·mL^{-1}) as well as different volumes of Tris-HCl buffer to obtain a 40 μL of final volume of the mixture solution. Then, the solution was incubated for 30 min at 37 °C with gentle shaking. After that, 151 μL NaAc-HAc buffer and 5 μL MnO_2 nanosheets solution (450 μM) were further added into the solution. The subsequent experimental operations were found to be consistent with the operation of optimization the concentration of MnO_2 nanosheets. The control experiments were conducted in a similar way, except that no ALP was added. All the experiments were repeated for three times.

Assays of ALP activity

For the detection of ALP, 10 μL AAP (2 mM) and different concentrations of ALP were mixed together and diluted to 40 μL with Tris-HCl buffer. Then, the solution was incubated at 37 °C for 30 min with gentle shaking. Subsequently, 151 μL NaAc-HAc buffer and 5 μL MnO_2 nanosheets (450 μM) were added into the solution. After incubation at room temperature for 5 min, 4 μL of 8 mM TMB was added to the solution. Then, the solution was further incubated for 5 min in the dark. In the end, the solution was transferred into the 96-well plate and the UV-vis absorption intensity at 652 nm was recorded using the Varioskan LUX microplate reader. All the experiments were repeated for three times.

ALP activity assay in biological fluids samples

For the ALP activity assay in biological fluids, different concentrations of ALP were mixed with 4 μL fetal calf serum samples and 10 μL AAP (2 mM), as well as different volumes of Tris-HCl buffer to obtain a 40 μL of final volume of the

mixture solution. The subsequent experimental operations were performed as described above. Then, according the standard addition method, the recoveries were made by spiking a series of known activities of ALP in diluted fetal calf serum (2%). All the experiments were repeated for three times.

For serum samples detection, *Mus musculus* serum sample and rabbit serum sample were collected from our laboratory. The blood samples were obtained through venipuncture. The serum samples were obtained by centrifuging above blood samples at 10,000 rpm for 10 min. Then, the concentration of ALP in above serum samples was determined by the proposed colorimetric method and the commercial ALP-kit, respectively. Specifically, 4 μL of the mouse or rabbit serum sample was mixed with 26 μL of Tris-HCl buffer and 10 μL AAP (2 mM). Then, ALP activity detection was performed as described above and its concentration calculated according to the linear standard curves. All the experiments were repeated for three times.

Results and discussion

Choice of materials

Nanozymes are a class of inorganic nanomaterials with natural enzyme catalytic activity [21]. Most of nanomaterials, such as Cu-Pd/g-C_3N_4 [22], MVC-MOF [23] are regarded to be good peroxidase or oxidase-like activity. However, hydrogen peroxide (H_2O_2) participates in the oxidation of 3,3′,5,5′-tetramethylbenzidine (TMB) catalyzed by nanozyme with peroxidase-like activity. By contrast, nanomaterials with oxidase-like activity can avoid the participation of any H_2O_2 in this reaction [24]. In addition, the catalytic activity of nanozyme is related closely to their morphology. Two-dimensional (2D) nanomaterials can provide multiple catalytic active sites for a substrate due to their large surface, which improves catalytic performance [20]. Therefore, MnO_2 nanosheets with oxidase-like activity have become ideal nanomaterials to develop new colorimetric methods for the detection of ALP. Furthermore, the preparation process of MnO_2 nanosheets has the advantages of easy availability of raw materials, simply operation process and high cost-effectiveness. The characterizations of the MnO_2 nanosheets were shown in Electronic Supporting Material.

Feasibility study of colorimetric detecting ALP activity

To demonstrate the feasibility of this approach, several control experiments were investigated. Figure 2 indicates that the colorless substrate 3,3′,5,5′-tetramethylbenzidine (TMB) solution exhibits little absorption band in 400–750 nm (**curve a**). In the presence of MnO_2 nanosheets, however, the reaction solution

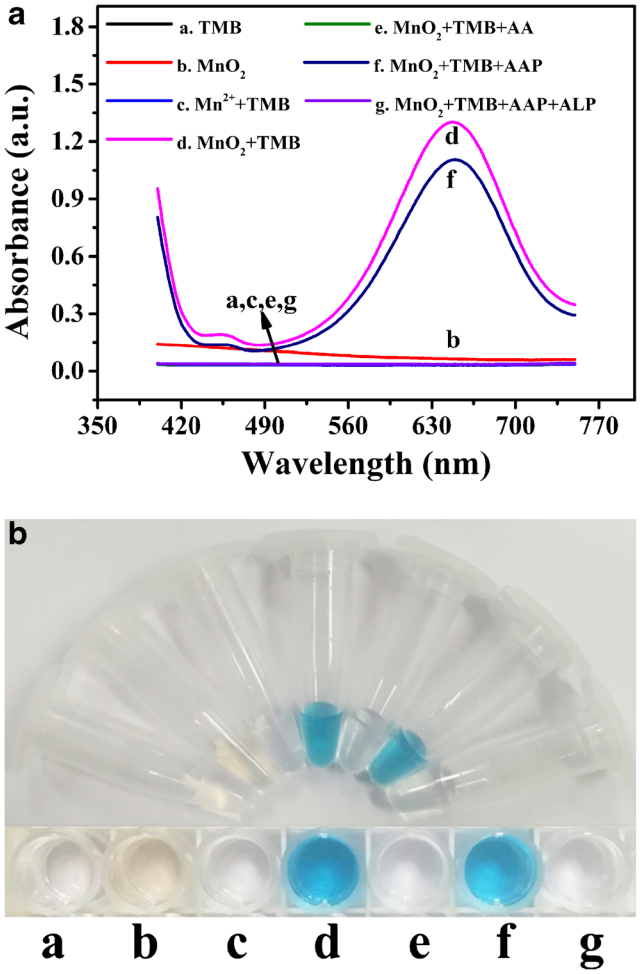


Fig. 2 (**a**) UV-vis absorption spectra of the mixtures; (**b**) the photographs corresponding to A. The reaction system were **a**: TMB, **b**: MnO_2 nanosheets, **c**: Mn^{2+} + TMB, **d**: MnO_2 nanosheets + TMB, **e**: MnO_2 nanosheets + TMB + AA, **f**: MnO_2 nanosheets + TMB + AAP, **g**: MnO_2 nanosheets + TMB + AAP + ALP, respectively. The experimental conditions: 160 μM TMB, 11.25 μM MnO_2 nanosheets, 100 μM AAP, 11.25 μM Mn^{2+}, 250 μM AA, 200 mU·mL^{-1} ALP, 200 mM NaAc-HAc buffer (pH 4.5)

shows a strong absorbance peak at 652 nm with change of color from colorless to blue, confirming the oxidase-mimic ability of MnO_2 nanosheets (Fig. 2, **curve d**). Alkaline phosphatase (ALP) has been reported to catalyze the dephosphorylation of ascorbic acid-2-phosphate (AAP) [4]. The MnO_2 nanosheets can be reduced into Mn^{2+} by the generating ascorbic acid (AA), thus losing its oxidase-mimic ability [25, 26]. To demonstrate the function of AA, the UV-vis spectra of the MnO_2 nanosheets in the absence and presence of AA were investigated. The characteristic absorption peak at 360 nm of the MnO_2 nanosheets completely disappears after adding AA, indicating that MnO_2 nanosheets have been reduced to Mn^{2+} by AA (Fig. S5, **curve c**). Then, the oxidation capacity of Mn^{2+} toward TMB was tested. As shown in Fig. 2, **curve c**, little changes of color

and absorbance of TMB are observed after the addition of Mn^{2+}, which indicates that TMB cannot be oxidized by Mn^{2+}. Therefore, TMB cannot be catalyzed by MnO_2 nanosheets in the presence of 250 μM of AA (Fig. 2, **curve e**). The high sensitivity response of MnO_2 nanosheets to AA facilitates the detection of ALP (Fig. S6). Figure 2, **curve f** shows that without ALP, MnO_2 nanosheets can still oxidize TMB in the presence of AAP. However, the maximum absorption peak of mixture at 652 nm disappears completely after the addition of ALP (Fig. 2, **curve g**). These results confirm the feasibly of this developed colorimetric method for ALP activity detection.

Optimization of detection strategy

To develop a colorimetric assay for ALP analysis with excellent performance, the concentration of MnO_2 nanosheets and AAP were optimized. The changing value of absorbance intensity at 652 nm (▵A) was used to achieve the optimization ($\triangle A = A_0 - A$, where A_0 and A represent the absorbance intensity at 652 nm of the proposed colorimetric method in the absence and presence of ALP, respectively). MnO_2 nanosheets, as oxidase-like mimic, directly affected the sensitivity of the constructed colorimetric method. Figure 3a illustrates the effect of different concentrations of MnO_2 nanosheets on the ▵A. The ▵A increased rapidly with the increasing concentration of MnO_2 nanosheets from 8.96 to 11.25 μM, and then it was significantly decreased with further increasing the concentration of MnO_2 nanosheets. Therefore, 11.25 μM of MnO_2 nanosheets was utilized as the optimal condition for subsequent experiments. AAP, as the substrate of ALP, was found to be closely related to the formation of AA, which consequently affected the degradation of MnO_2 nanosheets. The ▵A increased rapidly with the increasing concentration of AAP from 20 to 100 μM, and then reached a plateau (Fig. 3b). Therefore, 100 μM of AAP was selected as the optimal concentration.

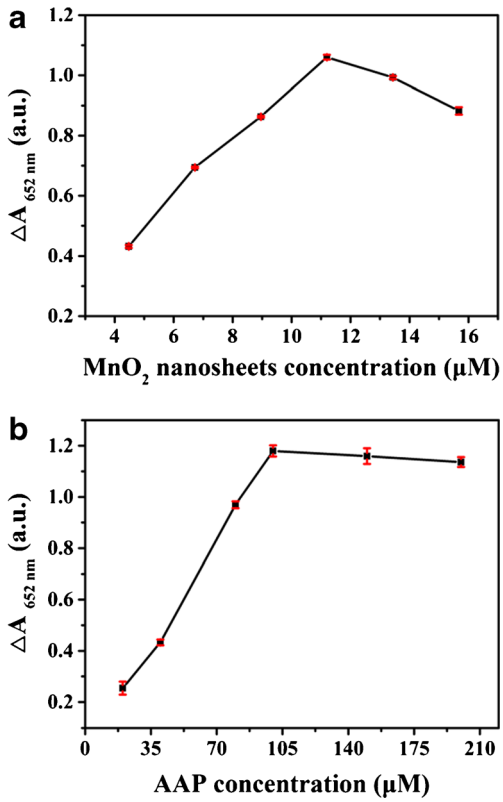


Fig. 3 Optimization of the concentration of MnO_2 nanosheets (**a**) and AAP (**b**) of this colorimetric assay. The error bars illustrate the standard deviations of three replicate measurements. The experimental conditions: 160 μM TMB, 200 $mU \cdot mL^{-1}$ ALP, 200 mM NaAc-HAc buffer (pH 4.5), 50 mM Tris-HCl (pH 9.0), absorbance 652 nm

The detection of ALP activity

Under the optimized experimental conditions, the feasibility of this colorimetric method for sensitive detection of ALP was investigated. As shown in Fig. 4a, the color of the solution is significantly faded from blue to colorless with the increasing activity of ALP, indicating that the semi-quantitative analysis of ALP activity can be easily achieved through visualization. As well, the absorbance intensity at 652 nm is decreased gradually (Fig. 4b). The ▵A exhibits a good linear relationship with the concentration of ALP ($R^2 = 0.9974$) in the range of 0.05 to 10 m-units per mL ($mU \cdot mL^{-1}$) (Fig. 4c). At the same time, the linear regression equation was $\triangle A = 0.0293\ x + 0.0026$ (x was the concentration of ALP), while the detection limit was found to be 0.05 $mU \cdot mL^{-1}$ according to the calculation of three times standard deviation over the blank response. The results are comparable or slightly lower than the previously reported methods (Table 1). Therefore, the MnO_2 nanosheets, as nanozymes, can be used for sensitively ALP determination.

Selectivity study

To evaluate the selectivity of the method, some other biological species such as bovine serum albumin (BSA), horseradish peroxidase (HRP), glucose oxidase (GOx), glucose (Glu), urea, L-cysteine (Cys) and glutathione (GHS) were studied, respectively. As displayed in Fig. 5a, the absorbance intensity of the reaction solution at 652 nm is reduced to the minimum only in the presence of ALP. In contrast, BSA, HRP, GOx, Glu and urea induce negligible changes of the absorbance intensity. It should be noted that, Cys and GSH bring about a decrease in absorbance intensity at 652 nm. The reason for this phenomenon can be attributed to the fact that the reducing

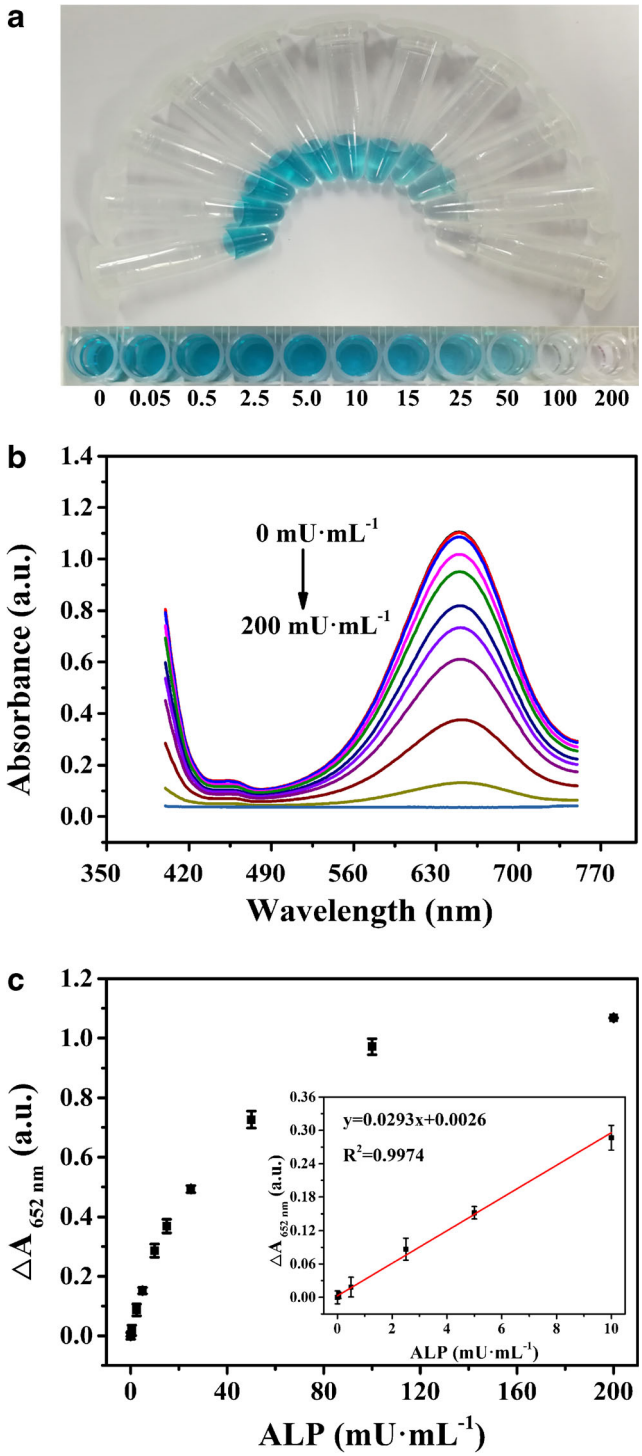


Fig. 4 Color changes (**a**) and absorption spectra (**b**) of MnO_2-TMB-AAP mixed solution induced by different activity of ALP. (**c**) The relationship between the changing value of absorbance intensity at 652 nm and the ALP concentration. Inset: calibration plot of the changing value of absorbance intensity at 652 nm versus concentration of ALP. The error bars illustrate the standard deviations of three replicate measurements. The experimental conditions: 160 μM TMB, 11.25 μM MnO_2 nanosheets, 100 μM AAP, 200 mM NaAc-HAc buffer (pH 4.5), 50 mM Tris-HCl (pH 9.0), absorbance 652 nm

Table 1 Comparison of recently reported colorimetric methods for ALP determination

Material	LOD ($mU{\cdot}mL^{-1}$)	Linear range ($mU{\cdot}mL^{-1}$)	Ref.
Fe(II)-phenanthroline complex	0.94	0–220	[6]
Cu(II)-phenanthroline complex	1.25	0–200	[27]
Gold nanoclusters	0.5	0.5–100	[28]
Gold nanorod	3.3	5–100	[29]
Gold nanoparticle	Not given	5–100	[30]
Gold nanoparticle	1.2×10^{-6}	5×10^{-6}-5×10^{-4}	[31]
Ce(IV) ions	2.3	0–50 and 50–250	[8]
Cu(II) ions	0.84	20–200	[32]
Cu(II)-modulated G-quadruplex-based DNAzymes	0.07	0.07–300	[33]
Cu(II)-metal organic frameworks	0.19	1–34	[3]
Citric acid-capped Prussian Blue nanocubes	0.23	0.6–6	[34]
CoOOH nanoflakes	0.032	0.04–160	[35]
MnO_2 nanosheets	0.05	0.05–10	This work

ability of Cys and GSH promotes the degradation of MnO_2 nanosheets. As exhibited in Fig. 5b, the absorbance signal response generating by ALP exhibits a maximum △A when compared to the other interfering substances. In addition, the color of reaction solution is nearly colorless in the presence of ALP, while other biological species caused little color changes (Fig. 4c, **Inset**). This result indicates that although the MnO_2 nanosheets-based colorimetric assay can be negatively affected by the existence of reducing species in the serum samples, the method still shows selectivity for the detection of ALP.

ALP activity assay in biological fluids samples

To investigate the applicability of the MnO_2 nanosheets-based colorimetric assay in biological fluids sample analysis, the activity of ALP was determined in 2% fetal calf serum samples. By testing with the commercial ALP-kit, it was found that it contained 0.87 $mU{\cdot}mL^{-1}$ of ALP in 2% fetal calf serum. The sensitivity of this method to ALP in complex samples was verified by spiking different concentrations of ALP into 2% fetal calf serum samples. With the incremental introduction of ALP, the decreased absorbance intensity at 652 nm was accompanied by visual fading of the blue color in the reaction system (Fig. 6a, b). Besides, the △A and the activity of ALP still exhibits a good linear relationship in the range of 0.87 to 10.87 $mU{\cdot}mL^{-1}$ with a R^2 of 0.9865 (Fig. 6c). According to the standard addition method, the recoveries were made by

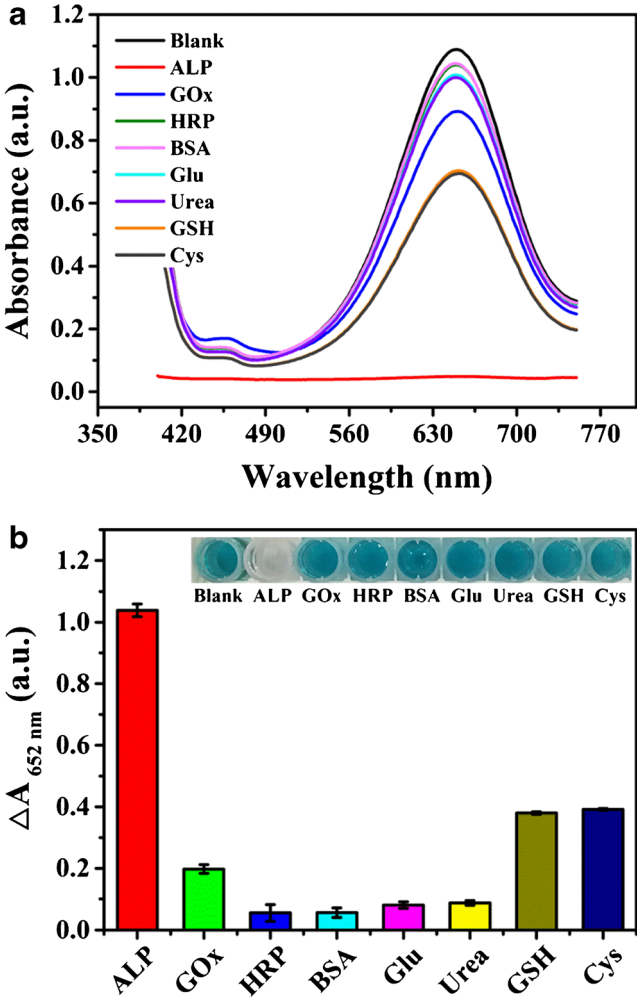


Fig. 5 **a** Absorption spectra of MnO_2-TMB-AAP mixed solution responding to ALP (200 mU·mL^{-1}), GOx (200 mU·mL^{-1}), HRP (200 mU·mL^{-1}), BSA (17.6 mg·L^{-1}), Glu (5 μM), urea (5 μM), GSH (5 μM) and Cys (5 μM), respectively. **b** Histogram of the changing value of absorbance intensity at 652 nm of different biological species. Insert: Photograph of the colorimetric system with different biological species. The error bars illustrates the standard deviations of three replicate measurements. The experimental conditions: 160 μM TMB, 11.25 μM MnO_2 nanosheets, 100 μM AAP, 200 mM NaAc-HAc buffer (pH 4.5), 50 mM Tris-HCl (pH 9.0), absorbance 652 nm

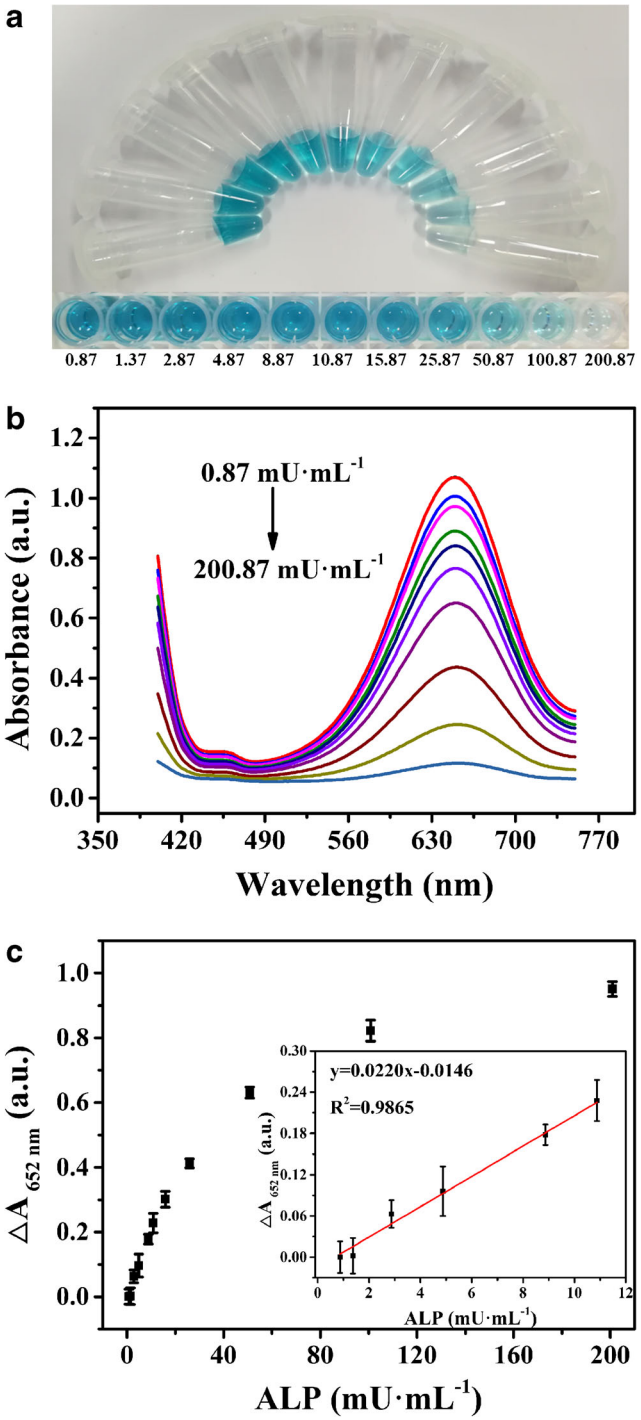


Fig. 6 Color changes (**a**) and absorption spectra (**b**) of MnO_2-TMB-AAP mixed solution induced by different concentration of ALP in 2% fetal calf serum. (**c**) The relationship between the changing value of absorbance intensity at 652 nm and the ALP concentration in 2% fetal calf serum. Inset: calibration plot of the changing value of absorbance intensity at 652 nm versus concentration of ALP in 2% fetal calf serum. The error bars illustrate the standard deviations of three replicate measurements. The experimental conditions: 160 μM TMB, 11.25 μM MnO_2 nanosheets, 100 μM AAP, 200 mM NaAc-HAc buffer (pH 4.5), 50 mM Tris-HCl (pH 9.0), absorbance 652 nm

spiking a series of known activities of ALP in diluted fetal calf serum (2%). As summarized in Table 2, recoveries are obtained ranging from 98.33 to 101.24% and the relative standard deviations (RSD) are lower than 7.76%. The results suggest that the method has potential applicability for the detection of ALP in biological fluids samples.

Furthermore, to test the reliability of the proposed method for the detection of ALP in real samples, ALP activity in real serum samples from two kinds of animals were analyzed with the proposed method and the commercial ALP-kit, respectively. **Table S1** displays that the differences in the results of these two methods are less than 5%. These results clearly demonstrate satisfactory performance for real sample analysis of the proposed MnO_2 nanosheets-based colorimetric method.

Table 2 Determination of ALP activities in 2% fetal calf serum samples (mean ± SD, $n = 3$)

Sample	ALP concentration in 2% fetal calf serum ($mU \cdot mL^{-1}$)	Added ($mU \cdot mL^{-1}$)	Found ($mU \cdot mL^{-1}$)	RSD (100%)	Recovery (%)
1	0.87	0.75	1.61 ± 0.13	7.76	98.33
2		5.00	5.82 ± 0.31	5.39	99.03
3		10.00	11.00 ± 0.71	6.48	101.24

Conclusion

Conclusively, on the basis of the enzymatic regulation of oxidase-mimic activity of MnO_2 nanosheets, a facile and sensitive colorimetric method is carried out to detect alkaline phosphatase (ALP) activity. ALP can catalyze the hydrolysis of AAP to ascorbic acid. This product triggers the decomposition of MnO_2 nanosheets by reducing MnO_2 to Mn^{2+}, thereby weakening the enzyme mimicking activity of the MnO_2 nanosheets and causing a drop in absorbance of the sensing system. Therefore, the sensitive detection of ALP can be achieved through the change of absorbance intensity. However, the existences of reducing species in the serum samples can affect colorimetric detection. To investigate the accuracy and reliability of this detection method, spiked recovery experiments in 2% fetal calf serum and ALP detection in real samples were performed. Overall, the excellent performance for serum samples analysis confirms this method′s great promise for the quantitative determination of ALP in clinical diagnosis. More importantly, this work provides a new insight for application of MnO_2 nanosheets in constructing biosensors.

Acknowledgements The authors thank the National Natural Science Foundation of China (No. 21405125), the Natural Science Foundation Project of CQ (No. cstc2018jscx-msybX0263) and the Fundamental Research Funds for the Central Universities (No. XDJK2019C026) for kindly support. In addition, the authors also thank China Agriculture Research System (No. CARS-27), National Risk Assessment Program for Agricultural Products Quality and Safety (No. GJFP2019003 and GJFP2019013) for financial support.

Compliance with ethical standards The author(s) declare that they have no competing interests. All procedures performed in studies involving animals were in accordance with the ethical standards of Chinese laws and guidelines (GKFCZ2001545).

References

1. Millan JL (2006) Alkaline phosphatases : structure, substrate specificity and functional relatedness to other members of a large superfamily of enzymes. Purinergic Signal 2(2):335–341
2. Ma JL, Yin BC, Wu X, Ye BC (2016) Copper-mediated DNA-Scaffolded silver nanocluster on-off switch for detection of pyrophosphate and alkaline phosphatase. Anal Chem 88(18):9219–9225
3. Wang C, Gao J, Cao Y, Tan H (2018) Colorimetric logic gate for alkaline phosphatase based on copper (II)-based metal-organic frameworks with peroxidase-like activity. Anal Chim Acta 1004: 74–81
4. He Y, Jiao B (2017) Determination of the activity of alkaline phosphatase based on the use of ssDNA-templated fluorescent silver nanoclusters and on enzyme-triggered silver reduction. Microchim Acta 184(10):4167–4173
5. Liu X, Fan N, Wu L, Wu C, Zhou Y, Li P, Tang B (2018) Lighting up alkaline phosphatase in drug-induced liver injury using a new chemiluminescence resonance energy transfer nanoprobe. Chem Commun (Camb) 54(88):12479–12482
6. Hu Q, Zhou B, Dang P, Li L, Kong J, Zhang X (2017) Facile colorimetric assay of alkaline phosphatase activity using Fe (II)-phenanthroline reporter. Anal Chim Acta 950:170–177
7. Zhang Z, Chen Z, Wang S, Cheng F, Chen L (2015) Iodine-mediated etching of gold Nanorods for Plasmonic ELISA based on colorimetric detection of alkaline phosphatase. ACS Appl Mater Inter 7(50):27639–27645
8. Song H, Wang H, Li X, Peng Y, Pan J, Niu X (2018) Sensitive and selective colorimetric detection of alkaline phosphatase activity based on phosphate anion-quenched oxidase-mimicking activity of Ce (IV) ions. Anal Chim Acta 1044:154–161
9. Wu S, Duan N, Qiu Y, Li J, Wang Z (2017) Colorimetric aptasensor for the detection of salmonella enterica serovar typhimurium using $ZnFe_2O_4$-reduced graphene oxide nanostructures as an effective peroxidase mimetics. Int J Food Microbiol 261:42–48
10. Zhao Z, Fan H, Zhou G, Bai H, Liang H, Wang R, Zhang X, Tan W (2014) Activatable fluorescence/MRI bimodal platform for tumor cell imaging via MnO_2 nanosheet-aptamer nanoprobe. J Am Chem Soc 136(32):11220–11223
11. Han L, Zhang H, Chen D, Li F (2018) Protein-directed metal oxide Nanoflakes with tandem enzyme-like characteristics: colorimetric glucose sensing based on one-pot enzyme-free Cascade catalysis. Adv Funct Mater 28(17):1800018
12. He L, Lu Y, Wang F, Jing W, Chen Y, Liu Y (2018) Colorimetric sensing of silver ions based on glutathione-mediated MnO_2 nanosheets. Sensor Actuat B-Chem 254:468–474
13. Xiao T, Sun J, Zhao J, Wang S, Liu G, Yang X (2018) FRET effect between fluorescent Polydopamine nanoparticles and MnO_2 Nanosheets and its application for sensitive sensing of alkaline phosphatase. ACS Appl Mater Inter 10(7):6560–6569
14. Ge J, Cai R, Chen X, Wu Q, Zhang L, Jiang Y, Cui C, Wan S, Tan W (2019) Facile approach to prepare HSA-templated MnO_2 nanosheets as oxidase mimic for colorimetric detection of glutathione. Talanta 195:40–45
15. Yan X, Song Y, Zhu C, Li H, Du D, Su X, Lin Y (2018) MnO_2 Nanosheet-carbon dots sensing platform for sensitive detection of organophosphorus pesticides. Anal Chem 90(4):2618–2624
16. Ge J, Xing K, Geng X, Hu YL, Shen XP, Zhang L, Li ZH (2018) Human serum albumin templated MnO_2 nanosheets are oxidase mimics for colorimetric determination of hydrogen peroxide and for enzymatic determination of glucose. Mikrochim Acta 185(12): 559
17. Liu J, Meng L, Fei Z, Dyson PJ, Zhang L (2018) On the origin of the synergy between the Pt nanoparticles and MnO_2 nanosheets in wonton-like 3D nanozyme oxidase mimics. Biosens Bioelectron 121:159–165
18. Sun Y, Tan H, Li Y (2018) A colorimetric assay for acetylcholinesterase activity and inhibitor screening based on the thiocholine-induced inhibition of the oxidative power of MnO_2 nanosheets on 3,3′,5,5′-tetramethylbenzidine. Mikrochim Acta 185(10):446

19. He Y, Wang C, Zhao Q, Zhang Y, Chen A, Pang J, Fang Q, Cui Y, Jiao B (2017) Facile and sensitive fluorescence sensing of alkaline phosphatase activity using NMM/G-quadruplex. Talanta 172:171–175
20. Liu J, Meng L, Fei Z, Dyson PJ, Jing X, Liu X (2017) MnO_2 nanosheets as an artificial enzyme to mimic oxidase for rapid and sensitive detection of glutathione. Biosens Bioelectron 90:69–74
21. Wei H, Wang E (2013) Nanomaterials with enzyme-like characteristics (nanozymes): next-generation artificial enzymes. Chem Soc Rev 42(14):6060–6093
22. Darabdhara G, Boruah PK, Das MR (2018) Colorimetric determination of glucose in solution and via the use of a paper strip by exploiting the peroxidase and oxidase mimicking activity of bimetallic Cu-Pd nanoparticles deposited on reduced graphene oxide, graphitic carbon nitride, or MoS_2 nanosheets. Microchim Acta 186(1)
23. Wang C, Tang G, Tan H (2018) Colorimetric determination of mercury (II) via the inhibition by ssDNA of the oxidase-like activity of a mixed valence state cerium-based metal-organic framework. Mikrochim Acta 185(10):475
24. Yan X, Song Y, Wu X, Zhu C, Su X, Du D, Lin Y (2017) Oxidase-mimicking activity of ultrathin MnO_2 nanosheets in colorimetric assay of acetylcholinesterase activity. Nanoscale 9(6):2317–2323
25. Na W, Li N, Xingguang S (2018) Enzymatic growth of single-layer MnO2 nanosheets in situ: application to detect alkaline phosphatase and ascorbic acid in the presence of sulfanilic acid functionalized graphene quantum dots. Sensor Actuat B-Chem 274:172–179
26. He L, Wang F, Chen Y, Liu Y (2018) Rapid and sensitive colorimetric detection of ascorbic acid in food based on the intrinsic oxidase-like activity of MnO_2 nanosheets. Luminescence 33(1): 145–152
27. Hu Q, He M, Mei Y, Feng W, Jing S, Kong J, Zhang X (2017) Sensitive and selective colorimetric assay of alkaline phosphatase activity with Cu (II)-phenanthroline complex. Talanta 163:146–152
28. Han X, Han M, Ma L, Qu F, Kong RM, Qu F (2019) Self-assembled gold nanoclusters for fluorescence turn-on and colorimetric dual-readout detection of alkaline phosphatase activity via DCIP-mediated fluorescence resonance energy transfer. Talanta 194:55–62
29. Gao Z, Deng K, Wang XD, Miro M, Tang D (2014) High-resolution colorimetric assay for rapid visual readout of phosphatase activity based on gold/silver core/shell nanorod. ACS Appl Mater Inter 6(20):18243–18250
30. Lin C, Zheng H, Sun M, Guo Y, Luo F, Guo L, Qiu B, Lin Z, Chen G (2018) Highly sensitive colorimetric aptasensor for ochratoxin a detection based on enzyme-encapsulated liposome. Anal Chim Acta 1002:90–96
31. Zhou CH, Zi QJ, Wang J, Zhao WY, Cao Q (2018) Determination of alkaline phosphatase activity and of carcinoembryonic antigen by using a multicolor liquid crystal biosensor based on the controlled growth of silver nanoparticles. Mikrochim Acta 186(1):25
32. Yang J, Zheng L, Wang Y, Li W, Zhang J, Gu J, Fu Y (2016) Guanine-rich DNA-based peroxidase mimetics for colorimetric assays of alkaline phosphatase. Biosens Bioelectron 77:549–556
33. Tang Z, Zhang H, Ma C, Gu P, Zhang G, Wu K, Chen M, Wang K (2018) Colorimetric determination of the activity of alkaline phosphatase based on the use of cu (II)-modulated G-quadruplex-based DNAzymes. Mikrochim Acta 185(2):109
34. Wu T, Hou W, Ma Z, Liu M, Liu X, Zhang Y, Yao S (2019) Colorimetric determination of ascorbic acid and the activity of alkaline phosphatase based on the inhibition of the peroxidase-like activity of citric acid-capped Prussian blue nanocubes. Microchim Acta 186(2):123
35. Liu SG, Han L, Li N, Xiao N, Ju YJ, Li NB, Luo HQ (2018) A fluorescence and colorimetric dual-mode assay of alkaline phosphatase activity via destroying oxidase-like CoOOH nanoflakes. J Mater Chem B 6(18):2843–2850

Publisher's note Springer Nature remains neutral with regard to jurisdictional claims in published maps and institutional affiliations.